AIAA Journal

VOLUME 2 OCTOBER 1964 NUMBER 10

Effects of Species Diffusion and Heat Conduction on Nonequilibrium Flows behind Strong Shocks

Walter E. Gibson* and John D. Buckmaster†
Cornell Aeronautical Laboratory, Inc., Buffalo, N. Y.

The effects of species diffusion and heat conduction are investigated for nonequilibrium flows behind strong, one-dimensional shocks. The relaxation zone is analyzed separately from the shock transition zone for translational (and rotational) temperature. It is shown that transport processes effectively decrease the high concentration and temperature gradients occurring in the relaxation zone behind strong shocks. This specific nonequilibrium behavior is studied for both vibration and dissociation. Strong effects are noted at shock speeds of 20 kft/sec (for vibration) and 29 kft/sec (for dissociation). Preliminary results are also given for airflows with coupled chemistry. Furthermore, a method for including the effects of freestream dissociation is presented for flows involving transport processes. Applications to bow shock flows at high re-entry speeds are pointed out.

Nomenclature

a = mean thermal velocity
a' = scaling factor defined in Eqs. (40) and (41)
$A_0(F_m)$ = function defined in Eqs. (31)
b = viscosity coefficient defined in Eq. (19)
C = rate coefficient for a Lighthill gas
D = diffusion coefficient
$F(\alpha, h)$ = function defined in Eqs. (26)
h = enthalpy parameter defined in Eq. (22)
$\mathcal{G}(\alpha; \Lambda, h)$ = function defined in Eq. (38)
l' = relaxation length in Eq. (11)
n = number of collisions for relaxation
p = gas pressure
q = gas velocity
$\mathcal{R}$ = universal gas constant, equal to 8.32×10^7 cgs
s = temperature exponent of dissociation rate [see Eq. (23)]
Sc = Schmidt number, see Eq. (20)
T = gas temperature
T_d = characteristic temperature of dissociation for a Lighthill gas
T' = dimensionless temperature defined in Eq. (21)
V = shock speed
W = molecular weight
z = scaled slope of concentration profile, see Eq. (25)
α = dissociation fraction
β = function defined in Eqs. (6)
γ = adiabatic exponent immediately behind the translation zone
δ = collision diameter, Å
$\Delta(\alpha)$ = function defined in Eqs. (32)
ϵ = local concentration of species
$\tilde{\epsilon}$ = local equilibrium concentration of species
λ = mean free path
Λ = parameter defined in Eq. (24)
μ = gas viscosity
ρ = gas density
σ = distance from the downstream boundary of the translation zone ($\sigma_{SH} = 0$)
σ' = distance variable defined in Eqs. (6)
Σ = equal to $\sigma'\Lambda^{1/2}$, see Eq. (37)
τ = relaxation time, see Eq. (4)
$\Omega^{2,2}$ = collision integral, see Eq. (19)

Subscripts

SH = denotes properties measured immediately behind the translation zone
∞ = denotes freestream properties
$(\bar{\ })$ = denotes a solution obtained for $\alpha_\infty = 0$, see Eqs. (39) et seq.

1. Introduction

SHOCK wave structure has attracted much interest as the basic example of a high energy, nonequilibrium flow. Both elastic and inelastic collision processes are involved in the coupling of translational energy with rotation, vibration, and chemical reactions. The nature of the coupling depends on shock strength.

For weak shocks, elastic collisions are much more frequent than inelastic ones so that the gas reaches translational equilibrium across a comparatively narrow zone. In the present paper, this region of translational equilibration is called the "translation zone." At low temperatures, the

---

Received December 23, 1963; revision received July 6, 1964. The research reported in this paper has been sponsored by NASA under Contract No. NASr-119 with Cornell Aeronautical Laboratory. The authors are pleased to acknowledge the capable help of C. Rippey in the preparation of the paper. The computer program applied in Sec. 3 was written by S. R. Graczyk.

[*] Senior Scientist at Avco, Research and Advanced Development Division, Wilmington, Mass.

[†] Assistant Aeronautical Engineer, Aerodynamic Research Department. Associate Member AIAA.

narrow translation zone can be studied[1] independent of relaxation processes. The internal degrees of freedom remain frozen at their freestream values, and the controlling physical effect is the elastic exchange of kinetic energy and momentum. This situation has been described[1] by various approximate solutions of the Boltzmann equation. Furthermore, the zone where relaxation occurs involves a continuum, inviscid flow. The initial conditions for the various relaxation processes are specified by the state of the gas after the translational transition. Current studies of this zone at the Cornell Aeronautical Laboratory include the coupling between vibration and dissociation.[2]

At high temperatures, the extrapolation[1, 3] of experimental data indicates a rapid decrease of the relaxation times for vibration and dissociation in airflows. Then, the division of shock structure into translation and relaxation zones must be carefully checked. Two questions should be asked about the relaxation zone. Does it depend on the structure of the translation zone? Is the flow inviscid?

The first question is considered in Refs. 1 and 4–7. The estimates of Ref. 1 and the solutions of Refs. 4 and 5 suggest that relaxation of vibration and dissociation never develops before the end of the translation zone. Even rotational relaxation is independent of the structure of the translation zone, as demonstrated by the solution of Ref. 6. Further estimates given in Ref. 7 support these conclusions.

To answer the second question, one need only examine available inviscid solutions. For example, at a lunar re-entry speed,[8] the relaxation zone shows such extreme concentration gradients that species diffusion must become important. Concurrently, the translational temperature drops very fast because thermal energy is very rapidly transformed into chemical energy. As a result, heat conduction cannot be neglected. In such a noteworthy situation, species diffusion and heat conduction are enhanced by the nonequilibrium nature of the flow.

This situation is studied here. The effects of nonequilibrium flow were not included in previous studies concerned with electron diffusion ahead of the shock.[9, 10] Furthermore, species diffusion was neglected (zero Lewis number) in the early work of Ref. 4 which treats oxygen dissociation in air at a shock speed of 20 kft/sec. In the present paper, species diffusion and heat conduction are found to have important effects on the relaxation zone at shock speeds of 20 kft/sec or more, depending on the chemical species.

The model for a strong shock assumes that the translational transition is completed before any significant relaxation occurs. This is consistent with the previous results just discussed. However, species diffusion and heat conduction are now allowed in the relaxation zone. Analytic and numerical solutions are obtained for simplified chemical models. The upstream boundary of the relaxation zone is defined by matching the concentration profile with a pure diffusion solution. This latter solution applies within the translation zone, where relaxation rates are neglected by virtue of the basic assumption.

The analysis of the relaxation zone is further simplified by dropping terms of order ρ_∞/ρ_{SH}, ρ_∞ and ρ_{SH} being, respectively, the freestream density and the density immediately behind the translation zone. Thus, momentum flux and momentum transport are neglected as higher-order effects so that the pressure remains constant. Accordingly, pressure diffusion is not included. Thermal diffusion is also ignored, as suggested by the results of Ref. 11. The Lewis number is assumed to be one so that species diffusion and heat conduction are given equal importance. Hence, the gas enthalpy is not affected[12] by species diffusion and heat conduction, i.e., the enthalpy remains equal to its post translation zone value, to order $(\rho_\infty/\rho_{SH})^2$. Finally, it should be noted that continuum flow is assumed in the relaxation zone.

It is interesting to compare the present study with the work of Refs. 13 and 14. These references account for transport processes in blunt body flows with cold walls near the free molecule limit. Then, nonequilibrium relaxation processes are not an essential feature of the problem. In fact, wall cooling depresses the reaction rates and effectively cancels the specific nonequilibrium behavior analyzed here. Species diffusion is important in Ref. 14 because of large mean free paths rather than because of high concentration gradients. In both Ref. 14 and the present paper, it is shown that upstream diffusion creates finite concentrations of excited species immediately behind the translation zone.

The rest of the paper comprises three sections. Section 2 gives the solution for a linearized model which displays the effect of species diffusion in a simple manner. Section 3 is devoted to a nonlinear theory for the Lighthill gas[15] including both species diffusion and heat conduction. Analytic and numerical solutions are obtained. The subtraction rule of Ref. 16 for freestream dissociation is extended to flows involving diffusion and conduction. Finally, Sec. 4 presents the conclusions. Applications to air flows with coupled chemistry and to blunt body flows are noted in Secs. 3 and 4. Reference 7 may be consulted for the mathematical details.

2. Linearized Theory

This section involves a single, linearized rate equation with species diffusion. The rate equation is analyzed behind the translation zone of a normal shock where the gas is assumed to be in translational equilibrium.‡ The results demonstrate the importance of species diffusion when the reaction rate is high. They are applied to vibrational relaxation in oxygen and nitrogen.

2.1 Flow Model

The one-dimensional flow behind the translation zone has a constant mass flux and a nearly uniform pressure

$$\rho q = \rho_\infty V_\infty \qquad p \approx p_{SH} = \frac{2}{\gamma_{SH}+1}\rho_\infty V_\infty{}^2 \tag{1}$$

Density changes are neglected in the linearized treatment of the relaxation zone, so that

$$\frac{\rho}{\rho_\infty} \simeq \frac{\rho_{SH}}{\rho_\infty} = \frac{\gamma_{SH}+1}{\gamma_{SH}-1} \tag{2}$$

In addition, the Schmidt number (or Prandtl number for diffusion) is set equal to one, although any constant value could be retained. Hence, the diffusion coefficient is

$$D = \mu/\rho \tag{3}$$

These assumptions simplify the analysis without compromising its general significance.

Upon inclusion of the diffusion term and application of Eq. (3), the relaxation equation is given by[17]

$$q\frac{d\epsilon}{d\sigma} - \frac{1}{\rho}\frac{d}{d\sigma}\left(\mu\frac{d\epsilon}{d\sigma}\right) = \frac{\tilde{\epsilon}-\epsilon}{\tau} \tag{4}$$

For vibrational relaxation, ϵ can represent the average vibrational energy of the gas, and Eq. (4) then accounts for the diffusion of vibrationally excited molecules (see Appendix A of Ref. 7). For a dissociation process, ϵ represents the atom concentration, and Eq. (4) includes the rate of atom diffusion. In both cases, the relaxation time τ is conveniently expressed in terms of an average number of collisions for relaxation, say n. The relaxation time τ is then given by $n\lambda/a$, where λ and a are the mean free path for elastic collisions and

---

‡ Rotational equilibrium is also assumed behind the translation zone, since rotational relaxation is not of particular interest here.

the mean thermal speed, respectively. Applying $\lambda = 2\mu/\rho a$ and $a = (8p/\pi\rho)^{1/2}$, one finds[6]

$$\tau = (\pi/4)(\mu/p)n \tag{5}$$

In the present analysis, $\tilde{\epsilon}$ and n are assumed constant (so that $\tilde{\epsilon} = \tilde{\epsilon}_{SH}$). This differs somewhat from the usual treatment[18] of linearized theory where the variations of $\tilde{\epsilon}$ are allowed. For vibrational relaxation, the linearization is justified in Appendix A of Ref. 7. For dissociation, the case of primary interest corresponds to high temperatures and low densities, i.e., to a situation where the local equilibrium is given by full dissociation, $\tilde{\epsilon} = 1$. Since the viscosity is a weak function of temperature and of ϵ, the assumption of constant n is only slightly less restrictive than that of constant relaxation time. Thus, the physical situation considered here is essentially that of relaxation in a heat bath. The heat bath solution is further examined in Sec. 3.

Two new variables are now introduced in Eq. (4), namely,

$$\beta = \frac{\epsilon}{\tilde{\epsilon}_{SH}} \qquad \sigma' = \int_0^{\sigma} \frac{q}{D}\, d\sigma \tag{6}$$

In the relaxation zone, σ' is equal to $\pi(\gamma_{SH} - 1)/8$ times the number of collisions experienced by a gas particle in going from 0 to σ. After application of Eqs. (1, 2, 5, and 6), Eq. (4) reduces to

$$\frac{d\beta}{d\sigma'} - \frac{d^2\beta}{d\sigma'^2} = \frac{8}{\pi(\gamma_{SH} - 1)}\,\frac{1}{n}\,(1 - \beta) \tag{7}$$

To determine a unique solution of Eq. (7), two boundary conditions are required. Let β_∞ be the freestream value for β, i.e., the value prescribed ahead of the translation zone. Far behind the translation zone, the rate process reaches equilibrium. Hence, one has

$$\begin{aligned} \sigma' &= -\infty: \beta = \beta_\infty = \epsilon_\infty/\tilde{\epsilon}_{SH} \\ \sigma' &= +\infty: \beta = 1 \end{aligned} \tag{8}$$

According to the present model, the relaxation rate is neglected upstream of the relaxation zone, i.e., within the translation zone and ahead of it. In this region, Eq. (7) can be integrated to give

$$\beta - \beta_\infty = d\beta/d\sigma' \text{ for } \sigma' \leq 0 \tag{9}$$

The solution of Eq. (9) predicts an exponential decay to β_∞ as $\sigma' \to -\infty$. At $\sigma' = 0$, the $\beta(\sigma')$ profile must be continuous. Thus, Eq. (9) and the second Eq. (8) provide the boundary conditions for the relaxation zone

$$\begin{aligned} \sigma' = 0:&\quad \beta_{SH} = \beta_\infty + (d\beta/d\sigma')_{SH} \\ \sigma' = +\infty:&\quad \beta = 1 \end{aligned} \tag{10}$$

The boundary condition at the shock includes a transport term $(d\beta/d\sigma')_{SH}$ that is analogous to that introduced in Ref. 14 for blunt body flows. Here, the transport effect arises specifically from the relaxation process rather than from the influence of a cold wall. As shown in Sec. 2.2, the inviscid limit $\beta_{SH} = \beta_\infty$ is recovered when n is large, i.e., when the relaxation time is long. For small n, the transport term in Eqs. (10) becomes much larger than β_∞, and the relaxation process is strongly modified by diffusion.

2.2 Solution of the Linearized Rate Equation

The exact solution of Eqs. (7) and (10) is

$$\frac{1 - \beta}{1 - \beta_{SH}} = \exp\left(-\frac{\sigma'}{l'}\right) \tag{11}$$

where the relaxation length l' and the concentration at the shock are found to be

$$\frac{1}{l'} = \frac{1}{2}\left\{\left[1 + \frac{32}{\pi(\gamma_{SH} - 1)}\,\frac{1}{n}\right]^{1/2} - 1\right\} \tag{12}$$

$$\frac{\beta_{SH} - \beta_\infty}{1 - \beta_\infty} = \frac{1}{1 + l'} \tag{13}$$

The effect of species diffusion is displayed by the dependence of l' and β_{SH} on n. If n is large, the diffusionless solution is recovered, corresponding to the neglect of $d^2\beta/d\sigma'^2$ in Eq. (7). Equations (12) and (13) then reduce to

$$l' \to (\pi/8)n(\gamma_{SH} - 1) \qquad \beta_{SH} \to \beta_\infty \text{ for } n \gg 1 \tag{14}$$

and exactly n collisions are required to decrease $(1 - \beta)/(1 - \beta_{SH})$ from 1 to $1/e$. On the other hand, if n is small, the diffusion term becomes dominant in the left-hand side of Eq. (7), giving

$$\begin{aligned} l' &\to 2\left[\frac{\pi}{8}\,n(\gamma_{SH} - 1)\right]^{1/2} \\ \beta_{SH} &\to \beta_\infty + \frac{1 - \beta_\infty}{1 + 2[(\pi/8)n(\gamma_{SH} - 1)]^{1/2}} \quad \text{for small } n \end{aligned} \tag{15}$$

Then, diffusion is an important mechanism, and the required number of collisions for relaxation is $[8n/\pi(\gamma_{SH} - 1)]^{1/2}$. Generally, as n decreases, both $1/l'$ and β_{SH} increase so that β increases for any fixed value of σ'. It also can be verified that diffusion decreases the concentration gradients.

As a realistic example, consider the range $10 \leq n \leq 100$ with $\gamma_{SH} = \frac{7}{5}$. For $n = 100$, one finds from Eq. (12) $l' = 16.67$ in excellent agreement with the first Eq. (14). For $n = 10$, the exact solution gives $l' = 2.27$, whereas the first Eq. (14) is still more accurate ($l' = 1.58$) than the strong diffusion value, $l' = 1.31$. Thus, the inviscid solution for the relaxation length is essentially valid for $n \geq 10$. On the other hand, the concentration at the shock is appreciably modified by diffusion since the factor $1/(1 + l')$ increases from 0.06 (for $n = 100$) to 0.30 (for $n = 10$). The conclusion is that, for $n \geq 10$, species diffusion modifies the inviscid profile effectively as an increase in freestream concentration. It should be recalled that heat conduction has no effect in the present model, since the relaxation time remains essentially constant.

The effective increase in freestream concentration is defined by Eq. (13). It is most marked when β_∞ is small, as occurs for a vibrationally cold or undissociated freestream. Furthermore, if n is kept the same, the ratio $(1 - \beta_{SH})/(1 - \beta_\infty)$ remains constant:

$$\frac{1 - \beta_{SH}(\beta_\infty)}{1 - \beta_\infty} = \frac{1 - \beta_{SH}(\beta_\infty')}{1 - \beta_\infty'} \tag{16}$$

for any choice of β_∞ and β_∞'. If β_∞ and β_∞' are small, Eq. (16) reduces to a subtraction rule similar to that of Ref. 16, namely,

$$\beta_{SH}(\beta_\infty) - \beta_\infty \approx \beta_{SH}(\beta_\infty') - \beta_\infty' \approx \beta_{SH}(0) \tag{17}$$

Equations (16) and (17) are extended in Sec. 3 for a nonlinear relaxation equation.

2.3 Vibrational Relaxation

The effect of species diffusion on vibrational relaxation behind a translational (and rotational) zone is now evaluated by applying the general solution, Eqs. (11) and (12). The validity of the flow model will also be studied.

The model for vibrational relaxation is that proposed in Ref. 18 for diatomic molecules. The rate equation is derived following Ref. 18 with, however, the inclusion of a transport term. This term describes the interdiffusion of vibrationally excited molecules. It is found to have an important effect at high temperatures.

As shown in Appendix A of Ref. 7, the rate equation is given by Eq. (7) with σ' and β defined as in Eqs. (6) and ϵ equal to the average vibrational energy. In fact, if both vibrational and translation temperatures are high, β is equal

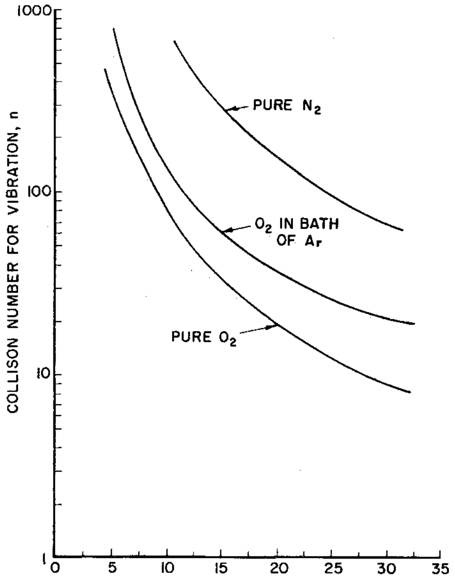

Fig. 1 Collision number for vibration.

to the ratio of vibrational to translational temperature (fully excited equilibrium vibration). Three gas mixtures are considered in the computations, namely, pure O_2, pure N_2, and O_2 in a bath of argon. The corresponding relaxation times are given by extrapolations of experimental data[19–21]:

$$\left.\begin{aligned} \tau_{O_2}p &= 1.6 \times 10^{-9} \exp\left[\frac{101.44}{T^{1/3}}\right] \\ \tau_{N_2}p &= 1.1 \times 10^{-11}T^{1/2} \exp\left[\frac{154}{T^{1/3}}\right] \\ \tau_{O_2\text{—}A} &= 1.1 \times 10^{-15}\, T^{5/6} \left[1 - \exp\left(-\frac{2228}{T}\right)\right]^{-1} \times \\ &\qquad \exp\left(\frac{1.04 \times 10^7}{T}\right)^{1/3} \end{aligned}\right\} \qquad (18)$$

In Eqs. (18), τ, p, and T are measured in seconds, atmospheres, and degrees Kelvin, respectively. The respective viscosity coefficients are approximated by the kinetic formula for a monatomic gas

$$\mu = b(T)^{1/2} \qquad b = \frac{2.7 \times 10^{-5}\, W_0^{1/2}}{\delta^2\Omega^{2,\,2}(T)} \qquad (19)$$

The data for the collision diameter δ (in angstrom) and the collision integral $\Omega^{2,\,2}$ are obtained from Ref. 16. Finally, γ_{SH} is set equal to $\frac{7}{5}$ for O_2 and N_2 and to $\frac{5}{3}$ for the argon bath.

As shown in Eq. (12), the governing parameter of the problem is the collision number, n. For vibrational relaxation of a given mixture, n depends only on the translational temperature [cf. Eqs. (5, 18, and 19)]. The function $n(T)$ is plotted in Fig. 1 for the three mixtures over a range of 5000°K $\leq T \leq$ 30,000°K. As T increases, n decreases rapidly because the increase of μ with temperature is overwhelmed by the strong decrease of τ. In fact, the curves of Fig. 1 are ordered according to the relaxation times, reflecting the decreasing collision efficiencies of O_2, A, and N_2 at a given temperature. It should be noted that n never falls below 10 in the range considered. This fact will be used below to justify the flow model adopted here.

Consistent with linearized theory, the value of n in Eqs. (12) and (13) is evaluated at the translational temperature for frozen vibration. This is rigorously correct for the argon bath and is found to be quite accurate for pure O_2 and N_2. Figure 2 shows the vibrational temperature $T_{V,\,SH}$ immediately behind the translation zone as a function of shock speed. The data correspond to a vibrational temperature T_{V_∞} = 300°K in the freestream. The computation is based on Eqs. (12) and (13). For inviscid flow, one has $T_{V,\,SH} = T_{V_\infty}$ = 300°K. The large effect of diffusion is apparent at shock speeds higher than 10^4 fps. As V_∞ increases, so does the ratio $T_{V,\,SH}/T_{SH}$, T_{SH} being the translational temperature at the shock. The significance of these results must, of course, be evaluated in view of the limited validity of the extrapolations used in Eqs. (18).

The order of the three curves in Fig. 2 should also be noted. At fixed shock speed, T_{SH} is essentially the same for O_2 and N_2, and the higher value for $T_{V,\,SH}$ (O_2) reflects only the lower value for n (O_2). However, T_{SH} is appreciably higher for the argon bath (higher values of γ_{SH} and W_0), and, consequently, the order of the three curves is different from that observed in Fig. 1.

Since large effects of diffusion are predicted for a realistic range of shock strengths, it appears worthwhile to study the flow model in more detail. This is done in Ref. 7 using the solutions obtained in Ref. 6. For the values of n indicated in Fig. 1, the present flow model is found to be accurate.

3. Analytic and Numerical Solutions for a Lighthill Gas

3.1 Introduction

The rate equation solved in the present section includes the variation of relaxation time with local temperature and concentration which was neglected in the linearized theory of Sec. 2. Thus, species diffusion and heat conduction are both involved in the solution. The problem treated is the dissociation of the Lighthill gas. Analytic solutions are given for a range of values of the rate coefficient which comprises the transition from an inviscid flow to one controlled by diffusion. Numerical solutions are also obtained. Air flows with coupled chemistry are also briefly discussed. The effect of dissociation in the freestream is considered, and the subtraction rule of Ref. 16 is extended to flows involving species diffusion.

3.2 Flow Model

Equations (1) remain valid behind the transport zone. However, in the present treatment, density variations in the relaxation zone are accounted for. Furthermore, the Schmidt number may now differ from one, so that the diffusion coefficient is given by

$$D = (\mu/\rho)Sc \qquad (20)$$

The Lewis number is assumed to be one. Thus, the enthalpy of the gas stays essentially constant ($q/V_\infty \ll 1$ in the relaxation zone) even when diffusion is important. The enthalpy of a Lighthill gas[15] is given by

$$h = (4 + \alpha)T' + \alpha \qquad T' = T/T_d \qquad (21)$$

with the enthalpy parameter

$$h = \frac{W_0 V_\infty^2}{2\mathcal{R}T_d} + \alpha_\infty \qquad (22)$$

The freestream concentration, α_∞ in Eq. (22), is set equal to zero in the solutions unless otherwise specified.

The viscosity coefficient is approximated by the value given in Eq. (19) for the undissociated gas. Indeed, the dependence of μ on α is not an important feature of reacting gas flows.[22] Furthermore, three-body recombination can be neglected in the relaxation equation[23] because the final equilibrium level reaches full dissociation at the high shock speeds of present interest. The dissociation rate is taken to be

$$C\rho(1 - \alpha)T^{-s} \exp[-(T_d/T)]$$

in conformity with the classical notation for a Lighthill gas. Equations (1, 6, 20, and 21) and the equation of state are combined with the relaxation equation, giving

$$\left.\begin{aligned} \frac{d\alpha}{d\sigma'} - \frac{d^2\alpha}{d\sigma'^2} &= \frac{CW_0{}^2V_\infty{}^2Sc}{\Re^2T_d{}^{s+2}}\,\mu\left(\frac{2}{\gamma_{SH}+1}\right)^2 \times \\ &\qquad \frac{1-\alpha}{(1+\alpha)^2}\,T'^{-(s+2)}\exp-\frac{1}{T'} \\ T' &= \frac{h-\alpha}{4+\alpha} \end{aligned}\right\} \qquad (23)$$

Since the local equilibrium concentration ($\bar{\epsilon}$ in Sec. 2) is equal to unity, β now becomes equal to the dissociation fraction α.

Next, Eq. (19) is substituted into Eqs. (23), and a controlling parameter of the problem is defined:

$$\Lambda = \frac{bCW_0{}^2V_\infty{}^2Sc}{\Re^2T_d{}^{s+3/2}} \qquad (24)$$

where, for simplicity, the viscosity coefficient b and the Schmidt number are assumed constant. As shown below, it is useful to scale the profile slope by $\Lambda^{1/2}$. Consequently, a new unknown function is introduced:

$$z = \Lambda^{-1/2}(d\alpha/d\sigma') \qquad (25)$$

Equations (23) reduce to a first-order differential equation for $z(\alpha; \Lambda, h)$ because the variable σ' is not explicitly involved. This simplification is due to the fact that the normal shock flow defines its own length scale. One obtains the basic formulation

$$\begin{aligned} [\Lambda^{-1/2} - (dz/d\alpha)]z &= (1-\alpha)F(\alpha, h) \\ F(\alpha, h) &\equiv \frac{1}{(1+\alpha)^2}\left(\frac{4+\alpha}{h-\alpha}\right)^{s+3/2}\exp\left(-\frac{4+\alpha}{h-\alpha}\right) \end{aligned} \qquad (26)$$

The boundary conditions for Eq. (26) are derived from Eqs. (10), namely,

$$\begin{aligned} &\sigma' = 0\colon\quad d\alpha/d\sigma' = z(\alpha_{SH}, \Lambda)\Lambda^{1/2} = \alpha_{SH} - \alpha_\infty \\ &\sigma' = \infty\colon\quad \alpha = 1 \qquad z = 0 \end{aligned} \qquad (27)$$

In fact, Eq. (26), being of first order in z, requires only one boundary condition that is chosen to be the second Eq. (27). Once the singular solution of Eq. (26) $\alpha = 1$, $z = 0$ is discarded, the second Eq. (27) specifies a unique, physically acceptable solution for $z(\alpha, \Lambda)$. The first Eq. (27) only serves to determine α_{SH}.

3.3 Analytic Solutions

Consider, first, the limiting cases of inviscid flow and of flow with strong diffusion. Since the parameter Λ is proportional to the ratio of the cross sections for inelastic (dissociation) and elastic collisions, small values of Λ correspond to a weak effect of diffusion. Indeed, for small Λ, Eqs. (26) yield the inviscid solution

$$z = (1-\alpha)\Lambda^{1/2}F(\alpha, h) \qquad (28)$$

On the other hand, for large Λ, Eqs. (26) reduce to

$$-z(dz/d\alpha) \approx (1-\alpha)F(\alpha, h) \qquad (29)$$

Thus, the Λ-dependence of z disappears for strong diffusion. This behavior motivated the choice made in Eq. (25).

To derive an analytic solution of Eqs. (26), it is helpful to start with a simple case where the rate function $F(\alpha, h)$ is approximated by a constant mean value

$$F(\alpha, h) \approx F_m \qquad (30)$$

The corresponding physical situation is that of dissociation in a heat bath [$F(\alpha, h)$ is primarily dependent on temperature that remains constant for the heat bath.] Equations (26) then have an exact solution

$$\begin{aligned} z &= (1-\alpha)A \\ A &= A_0(F_m) = \tfrac{1}{2}[(4F_m + \Lambda^{-1})^{1/2} - \Lambda^{-1/2}] \end{aligned} \qquad (31)$$

As expected, the function $A_0(F_m)$ is simply related to the relaxation length l' of the linearized theory [cf. Eq. (12)]. One has

$$l' = \frac{\Lambda^{-1/2}}{A_0F_m}$$

$$n = \frac{8}{\pi(\gamma-1)}\,\frac{1}{\Lambda F_m}$$

Equations (31) also apply when $F(\alpha, h)$ varies slowly with α, provided F_m is replaced by the local value $F(\alpha, h)$. A correction term of order $\partial F/\partial\alpha$ is easily included as follows. Equations (31) are substituted into Eqs. (26) giving an exact relation for A:

$$A - (F/A) + \Lambda^{-1/2} = (1-\alpha)(\partial A/\partial\alpha)$$

Next, using a perturbation expansion,

$$A = A_0(F) + \frac{(1-\alpha)A_0(F)\Lambda^{1/2}}{1 + 2A_0(F)\Lambda^{1/2}}\,\frac{\partial A_0}{\partial\alpha} + \ldots$$

or

$$\begin{aligned} z &= (1-\alpha)A_0[\alpha + \Delta(\alpha)] \\ \Delta(\alpha) &= \frac{(1-\alpha)A_0[F(\alpha, h)]\Lambda^{1/2}}{1 + 2A_0[F(\alpha, h)]\Lambda^{1/2}} \end{aligned} \qquad (32)$$

This result provides a simple analytic solution. For weak diffusion ($\Lambda \to 0$), Eqs. (32) agree with the exact solution up to order $\Lambda^{5/2}$. For strong diffusion ($\Lambda \gg 1$), Eqs. (32) are subject to an error of order $[\partial^2F(\alpha, h)/\partial\alpha^2]$, as may be checked by substitution into Eq. (29). In fact, Eqs. (32) are in good agreement with the exact numerical solution obtained below for $\Lambda \geq 1$. This is shown by Table 1 in which the analytic solution for $z(\alpha = 0, h)$ is compared with the exact solution ($h = 3.0$).

The maximum error of the approximate solution does not exceed 16%. For other values of α and h, the agreement is

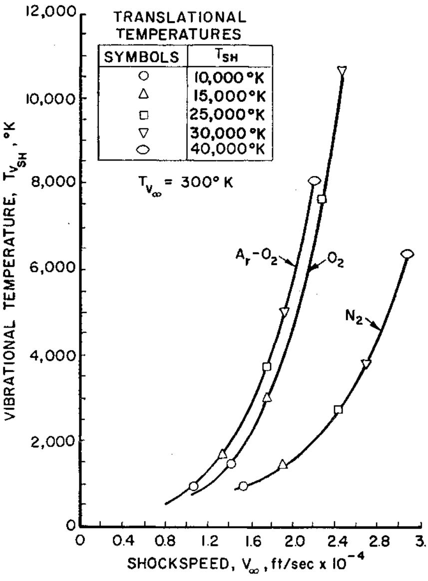

Fig. 2 Vibrational temperature behind translation zone.

Table 1 Comparsion of exact and approximate solutions

Λ	1	10	10^2	10^3	∞
$A_0[\Delta(0)]$	0.23	0.33	0.39	0.41	0.42
Exact	0.26	0.39	0.46	0.48	0.50

equally good. This is not surprising in view of the physical validity of the analytic solution. Indeed, at high enthalpies, neither the temperature nor the chemical rate vary strongly with α so that the heat bath approximation is valid. At low enthalpies where diffusion is less important, the inviscid solution is identically recovered by Eqs. (32).

In summary, the relaxation equation for nonequilibrium diffusive flow behind a normal shock has a simple analytic solution that describes accurately the transition from weak to strong diffusion effect as the rate coefficient is increased.

3.4 Exact Solutions and Results

Exact solutions for a Lighthill gas

The exact solution of Eqs. (26) is obtained by numerical integration starting from the equilibrium limit, $\alpha = 1$ with $A = z/(1 - \alpha)$ as an auxiliary unknown. For $\Lambda \geq 10$, the numerical scheme is found to be stable. For $\Lambda < 10$, a numerical instability arises near $\alpha = 1$. It is circumvented by applying Eqs. (32) over a small interval $\alpha_1 \leq \alpha \leq 1$. The effect of varying α_1 between 0.95 and 0.99 is found to be negligible.

Once $z(\alpha, h)$ is known, the concentration profile is obtained from

$$\frac{\sigma}{l} = \int_{\alpha_{SH}}^{\alpha} \frac{T'^{1/2}}{z} d\alpha \qquad l = \frac{\rho_\infty V_\infty(\Lambda)^{1/2}}{b(T_d)^{1/2}} \tag{33}$$

where α_{SH} is the concentration at the upstream boundary of the relaxation zone. Furthermore, α_{SH} is determined by the first Eq. (27).

Effect of diffusion for a Lighthill gas

The numerical solutions for $z(\alpha; \Lambda, h)$ are given in Fig. 3. The data have been computed for $h = 3$(e.g., $V_\infty = 28.5$ kft/sec in pure oxygen and $\alpha_\infty = 0$). The temperature exponent s in Eqs. (26) is set equal to zero as suggested by recent experimental results.[24] A large range of values of Λ is considered, so as to explore the parametric dependence of the solution. When the following values are substituted in Eqs. (19) and (24),

$$\delta = 3.5\ \text{Å} \qquad \Omega^{2,2} = 0.7 \qquad W_0 = 32 \qquad Sc = 1$$
$$C = 6 \times 10^{14}\ \text{cm}^3\text{-g}^{-1}\text{-sec}^{-1} \qquad T_d = 6 \times 10^4\ {}^\circ\text{K} \tag{34}$$

one finds

$$\Lambda = 82 \tag{35}$$

Actually, the choice of C in Eqs. (34) corresponds to O_2 dissociation in a bath of argon.[24] By analogy with the lower temperature case,[25] it is expected that O atoms would have a higher collision efficiency than argon, so that Eq. (35) may give a lower limit for Λ.

The dashed lines in Fig. 3 represent the inviscid solution, Eq. (28), and the dotted lines define the solution for pure diffusion, Eq. (9). The exact solutions including diffusion and relaxation effects are shown as full lines. Figure 3 demonstrates that diffusion is quite effective in smoothing out the concentration gradients, i.e., for a given $\Lambda \geq 10$, the exact solution is much smaller than the inviscid solution. In fact, z is a weak function of Λ for $\Lambda \geq 10^2$, so that the solution is essentially that obtained for strong diffusion [see Eq. (29) and the subsequent discussion]. On the other hand, the dashed and full curves in Fig. 3 agree comparatively well at $\Lambda = 1$, indicating that $\Lambda = 1$ defines a lower limit of the diffusion-controlled regime.

For the cases considered in Fig. 3, one finds appreciable concentrations immediately behind the translation zone:

$$\begin{aligned} \alpha_{SH} &= 0.17 \qquad \text{for } \Lambda = 1 \\ \alpha_{SH} &= 0.46 \qquad \text{for } \Lambda = 10 \end{aligned} \tag{36}$$

Thus, diffusion creates finite atom concentrations immediately behind the translation zone. This behavior is analyzed in Ref. 14 for a fully viscous shock layer with a cold wall. The present results show that species diffusion has a similar effect on normal-shock flows that do not involve heat losses.

The effect of finite concentrations at the shock on the concentration profiles is apparent from the full curves of Fig. 4. The curves are plotted against the scaled coordinate $\sigma'(\Lambda)^{1/2}$ for $\Lambda = 1$, 10, and 10^2 and $h = 3.0$ (same as in Fig. 3). The dashed curves represent the inviscid solutions. The solutions including diffusion and conduction are expressed in the form

$$\mathscr{S}(\alpha; \Lambda, h) - \mathscr{S}(\alpha_{SH}; \Lambda, h) = \sigma'(\Lambda)^{1/2} = \Sigma \tag{37}$$

where

$$\mathscr{S}(\alpha; \Lambda, h) = \int_0^{\alpha} \frac{d\alpha}{z(\alpha; \Lambda, h)} \tag{38}$$

In other words, the profiles $\alpha(\Sigma)$ are obtained by cutting off the basic profile

$$\mathscr{S}(\alpha; \Lambda, h) = \Sigma$$

at $\alpha \leq \alpha_{SH}$. This procedure should be compared to that applied in Ref. 1 to account for the effect of freestream dissociation on inviscid flows.

For $\Lambda = 1$, it is found that the function $\mathscr{S}$ agrees essentially with the inviscid solution $\mathscr{S}(\alpha, 0, h)$. Consequently, the diffusion profile can be obtained by cutting off the inviscid solution at $\alpha \leq \alpha_{SH}$. When diffusion is weak, it modifies the inviscid flow in the same manner as the presence of a finite atom concentration in the freestream. The strong effect of diffusion is apparent for $\Lambda = 10$ and 10^2. For fixed α, the comparison with the inviscid profiles shows that the concentration gradient is strongly reduced by diffusion.

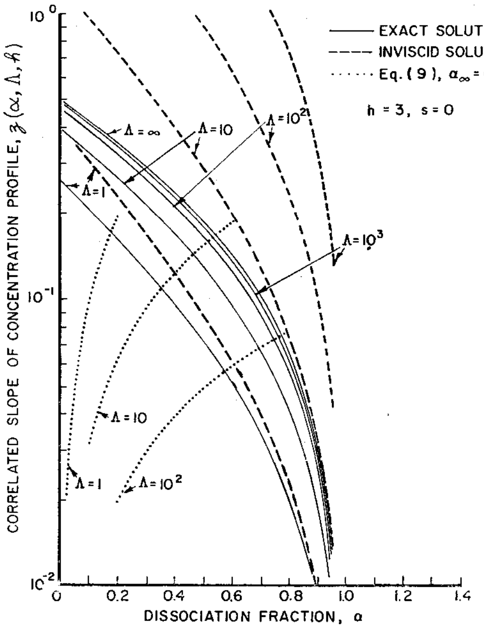

Fig. 3 Effect of diffusion on concentration gradients for a Lighthill gas.

For a fixed distance behind the transport shock, the dissociation fraction is, in general, strongly increased. However, the relaxation length for the variable $\sigma'(\Lambda)^{1/2}$ is not drastically modified by diffusion. Hence, the relaxation length can be estimated for practical purposes on the basis of the inviscid solution for the same value of Λ. Thus, the determination of the rate coefficient from a measurement of the relaxation time is not critically affected by species diffusion.

The foregoing results for a Lighthill gas agree essentially with those obtained from the linearized theory of Sec. 2. The only difference is that species diffusion and heat conduction have a stronger effect on profile shape in the nonlinear theory.

3.5 Applications to Airflows and to Flows with Dissociated Freestreams

Effect of diffusion for airflows

Strong shocks in air are considered in Ref. 7 (Appendix B). The shock speed assumed is 23 kft/sec. Electron diffusion is taken to be ambipolar, and the rates of Ref. 25 are used. Oxygen atom and temperature distributions are not modified by diffusion, but nitric oxide and electron distributions are strongly affected [see Figs. (B-1) and (B-2) of Ref. 7]. For instance, (NO) and (e^-) immediately behind the translation zone are increased to 2.5×10^{-3} and 10^{-5} moles per original mole, respectively, through upstream diffusion from the relaxation zone. These results are obtained from approximate solutions, and their validity should be verified on the basis of exact solutions.

Effect of freestream dissociation for a Lighthill gas

The effect of freestream dissociation on the nonequilibrium flow of a Lighthill gas with diffusion and conduction is analyzed in Ref. 7. A subtraction rule for freestream dissociation is derived. It is a direct extension of the results of Ref. 16 which were given for inviscid flow. One finds

$$\begin{aligned} &\alpha(\sigma'; h) - \alpha_{SH} \approx \bar{\alpha}(a'\sigma'; \bar{h}) - \bar{\alpha}_{SH} \\ &T(\sigma'; h) \approx \bar{T}\,(a'\sigma'; \bar{h}) \qquad \frac{\alpha_{SH} - \alpha_\infty}{\bar{\alpha}_{SH}} = a' \end{aligned} \tag{39}$$

where the scaling factor a' takes on different values depending on the importance of transport phenomena. Barred symbols denote a solution for $\alpha_\infty = 0$. For weak diffusion ($\Lambda \leq 1$), a' is equal to

$$a' = \frac{1 - \alpha_{SH}}{1 - \bar{\alpha}_{SH}} \frac{(1 + \bar{\alpha}_{SH})^2}{(1 + \alpha_{SH})^2} \frac{h - \alpha_\infty}{\bar{h}} \tag{40}$$

For strong diffusion ($\Lambda \gg 1$), one has

$$a' = \frac{1 - \alpha_{SH}}{1 - \bar{\alpha}_{SH}} \frac{1 + \bar{\alpha}_{SH}}{1 + \alpha_{SH}} \left(\frac{h - \alpha_\infty}{\bar{h}}\right)^{1/2} \tag{41}$$

In both cases, a' is independent of the rate coefficient, and the enthalpy h and $\bar{h}$ must be related by

$$h - \alpha_{SH} = \bar{h} - \bar{\alpha}_{SH} \tag{42a}$$

or

$$h = \bar{h} + \alpha_\infty + (a' - 1)\bar{\alpha}_{SH} \tag{42b}$$

These results are established by a straightforward extension[7] of the analysis of Ref. 16. One should note that, for $\bar{\alpha}_{SH} = 0$ (no diffusion), Eq. (42) reduces to the requirement of fixed velocity in the freestream.[16]

4. Concluding Remarks

The paper considers the effect of species diffusion and heat conduction on nonequilibrium gas flows behind strong shocks. In the present model, the shock wave is divided in two zones that are controlled by translational equilibration and relaxation processes, respectively. Within the translation zone, the gas achieves a high enthalpy by translational equilibration through elastic collisions without appreciable internal excitation. Within the relaxation zone inelastic collisions bring about internal excitation subject to species diffusion and heat conduction. The upstream boundary of the relaxation zone is determined by matching the concentration profile for the relaxation zone with the pure diffusion solution applicable within the translation zone.

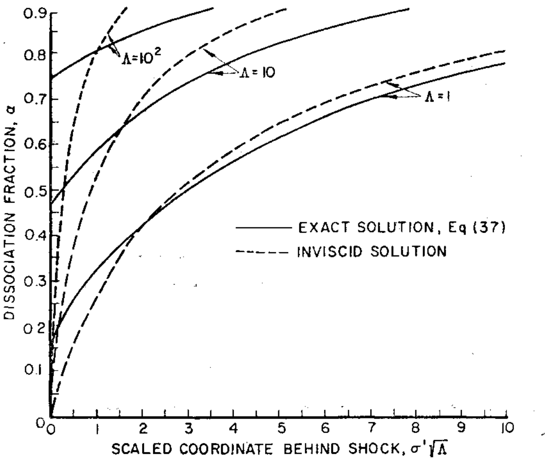

Fig. 4 Effect of diffusion on concentration profiles for a Lighthill gas.

The analysis is developed for two chemical models, vibrational relaxation and dissociation. Applications to airflows with coupled chemistry are indicated. The results show important effects of species diffusion and heat conduction at shock speeds above 20 kft/sec. Species diffusion and heat conduction strongly decrease the concentration gradients predicted by inviscid solutions for the relaxation zone. Furthermore, the diffusion of excited species establishes finite concentrations within the translation zone. On the other hand, the relaxation length is not appreciably modified.

The extent of the effects depends on the relaxation process. Vibrational relaxation is rather insensitive to heat conduction because of the small energy content involved and of the weak dependence of relaxation time on translational temperature. However, the diffusion of vibrationally excited molecules is a major effect at shock speeds as low as 20 kft/sec. For instance, the vibrational temperature immediately behind the translation zone in pure O_2 at 20 kft/sec is found to be 4000°K. The inviscid solution, however, predicts a vibrational temperature equal to the freestream value, namely, 300°K in the present example.

At 23 kft/sec in air, electron and nitric oxide distributions are strongly affected by diffusion[7]; atom and temperature distributions are not. Again, high molar concentrations are created immediately behind the translation zone, i.e., 10^{-5} moles per original mole for electrons and 2.5×10^{-3} for nitric oxide. Finally, at 29 kft/sec, the dissociation of pure O_2 is shown to be markedly influenced by both diffusion and conduction. Analytic and numerical solutions are given, and the effect of changing the rate coefficient is examined. A tenfold decrease of the rate coefficient from the presently used value does not materially reduce the importance of transport processes.

The subtraction rule of Ref. 16 for a dissociated freestream is extended to nonequilibrium flows involving species diffusion and heat conduction. In most cases, the effect of freestream dissociation on an inviscid flow is quite similar to that of transport processes. The analogy requires that the state of the gas be the same immediately behind the translation zone. Thus, the shock speed must be fixed, and the freestream dissociation must equal that created by species diffusion.

The full validity of the present results will become clearer with our increasing knowledge of high-temperature air chemistry. However, it is suggested that species diffusion and heat conduction should not be routinely neglected in the study of relaxation zones behind strong shocks. These effects should also play an important role in blunt-body flows near the bow shock even when the Reynolds number based on body radius is large.

References

[1] Talbot, L., "Survey of the shock structure problem," ARS J. **32,** 1009–1016 (1962).

[2] Treanor, C. E., "Vibrational relaxation effects in dissociation rate-constant measurements," Cornell Aeronautical Lab. Rept. AG-1729-A-1 (August 1962).

[3] Parker, J. G., "Rotational and vibrational relaxation in diatomic gases," Phys. Fluids **2,** 449–462 (1959).

[4] Gaitatzes, G. and Bloom, M. H., "On the interior of normal shocks according to continuum theory, including rate thermochemistry," Polytechnic Institute of Brooklyn, Aeronautical Research Lab. Rept. 65 (June 1961).

[5] Scala, S. M. and Talbot, L., "Shock wave structure with rotational and vibrational relaxation," General Electric Rept. Air Force Office of Scientific Research 1494, R62SD32 (October 1962).

[6] Talbot, L. and Scala, S. M., "Shock wave structure in a relaxing diatomic gas," *2nd International Symposium on Rarefied Gas Dynamics,* edited by L. Talbot (Academic Press, New York, 1961), pp. 603–622.

[7] Gibson, W. E. and Buckmaster, J. D., "The effects of species diffusion and heat conduction on nonequilibrium flows behind strong shocks," Cornell Aeronautical Lab. Rept. AG-1729-A-3 (October 1963).

[8] Eschenroeder, A. Q., Daiber, J. W., Golian, T. C., and Hertzberg, A., "Shock tunnel studies of high enthalpy ionized airflows," Cornell Aeronautical Lab. Rept. AF-1500-A-1, Air Force Office of Scientific Research 3025 (March 1962).

[9] Weymann, H. D., "Electron diffusion ahead of shock waves in argon," Maryland Univ., Institute for Fluid Dynamics and Applied Mathematics, TN BN-197, Air Force Office of Scientific Research AFOSR-TN-60-334 (March 1960).

[10] Wetzel, L., "Precursor effects and electron diffusion from a shock front," Phys. Fluids **5,** 824–830 (1962).

[11] Sherman, F. S., "Shock-wave structure in binary mixtures of chemically inert perfect gases," J. Fluid Mech. **8,** 465–480 (1960).

[12] Lees, L., "Convective heat transfer with mass addition and chemical reactions," *Third AGARD Combustion and Propulsion Panel Colloquium* (Pergamon Press, New York, 1958), pp. 451–498.

[13] Cheng, H. K., "Hypersonic shock-layer theory of the stagnation region at low Reynolds number," *Proceedings of the Heat Transfer and Fluid Mechanics Institute* (Stanford University Press, Stanford, Calif., 1961), pp. 161–175; also Cornell Aeronautical Lab. Rept. AF-1285-A-7 (April 1961).

[14] Cheng, H. K., "The blunt-body problem in hypersonic flow at low Reynolds number," IAS Preprint 63-92 (January 1963).

[15] Lighthill, M. J., "Dynamics of a dissociating gas, Part I. Equilibrium flow," J. Fluid Mech. **2,** 1–32 (1957).

[16] Gibson, W. E., "The effect of ambient dissociation on nonequilibrium shock layers," Cornell Aeronautical Lab. Rept. AD-1716-A-2 (September 1963).

[17] Penner, S. S., *Introduction to the Study of Chemical Reactions in Flow Systems* (Butterworths Scientific Publications, London, 1955), Chap. 2.

[18] Gibson, W. E. and Moore, F. K., "Acoustic propagation in a diatomic gas subject to thermal or chemical relaxation," Cornell Aeronautical Lab. Rept. HF-1056-A-2 (October 1958).

[19] Landau, L. D. and Teller, E., "Contribution to the theory of sound dispersion," Phys. Z. Sowjetunion **10,** 34 (1936).

[20] Blackman, V. H., "Vibrational relaxation in oxygen and nitrogen," J. Fluid Mech. **1,** 61–85 (1956).

[21] Camac, M., "O_2 vibration relaxation in oxygen-argon mixtures," J. Chem. Phys. **34,** 460–470 (1961).

[22] Moore, F. K., "On the viscosity of dissociated air," ARS J. **32,** 1415–1416 (1962).

[23] Gibson, W. E., "Dissociation scaling for nonequilibrium blunt-nose flows," ARS J. **32,** 285–287 (1962).

[24] Wray, K. L., "Shock-tube study of the O_2-Arrates of dissociation and vibrational relaxation," J. Chem. Phys. **37,** 1254–1263 (1962).

[25] Wray, K. L., "Chemical kinetics of high temperature air," *ARS Progress in Astronautics and Rocketry: Hypersonic Flow Research,* edited by F. R. Riddell (Academic Press, New York, 1962), pp. 181–204.

[26] Hall, J. G., Eschenroeder, A. Q., and Marrone, P. V., "Blunt-nose inviscid airflows with coupled nonequilibrium processes," J. Aerospace Sci. **29,** 1038–1051 (1962).